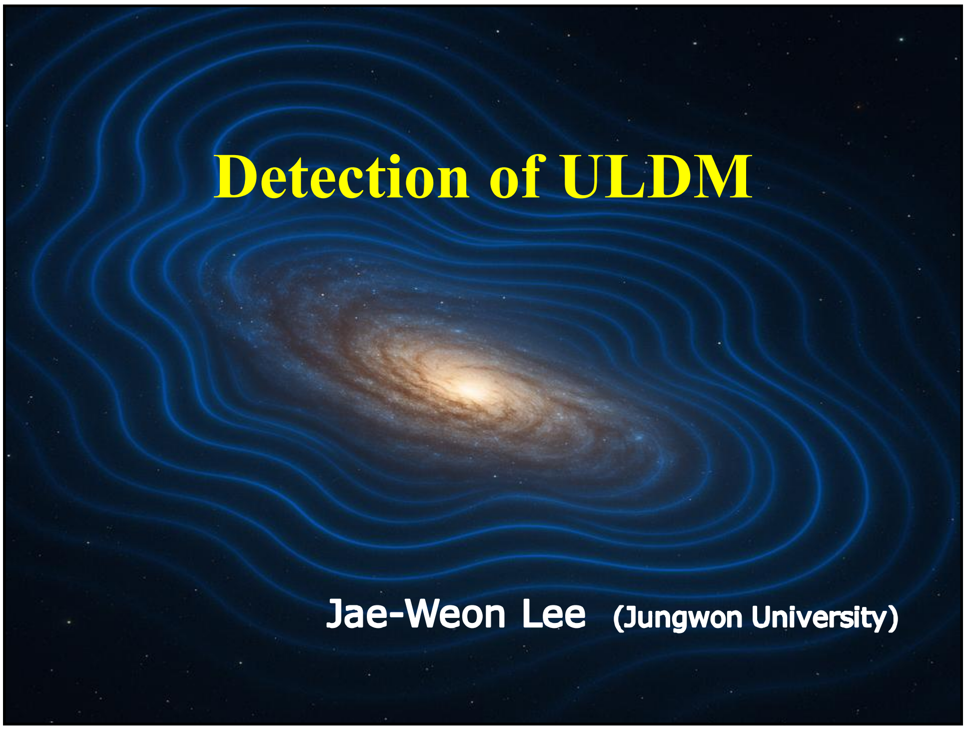

1

Outline

1. Constraints on ULDM (FDM)
   → only gravitationally
2. Constraints on SIULDM
   (TF limit)

2

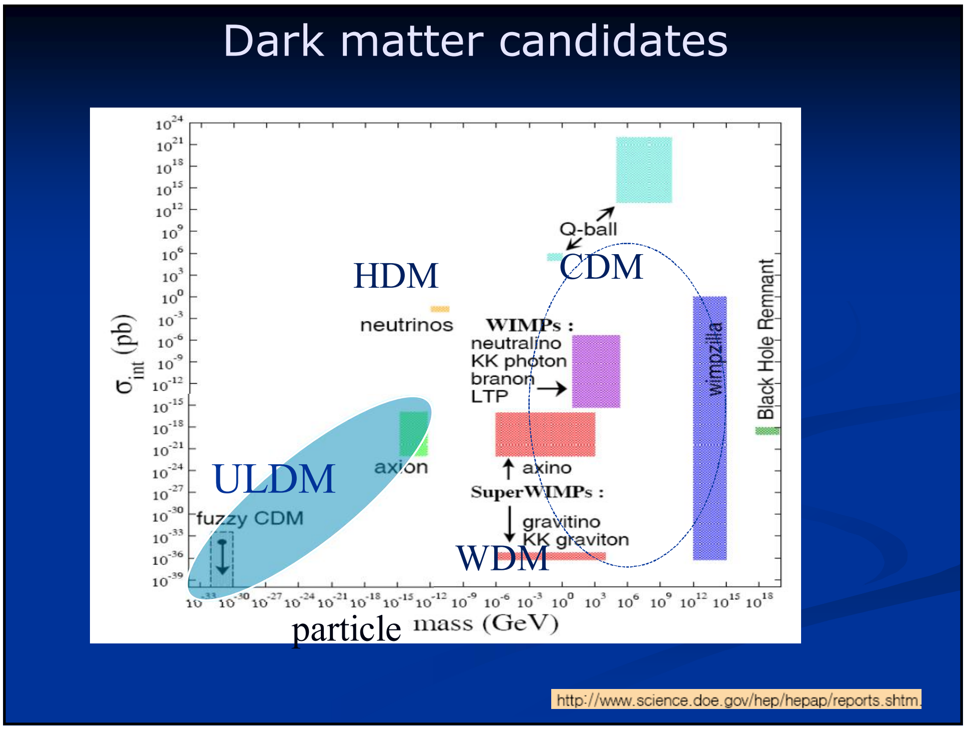
Dark matter candidates
σint (pb)
particle mass (GeV)
HDM
neutrinos
CDM
Q-ball
WIMPs :
neutralino
KK photon
branon
LTP
axion
SuperWIMPs :
gravitino
KK graviton
WDM
ULDM
fuzzy CDM
axion
wimpzilla
Black Hole Remnant
http://www.science.doe.gov/hep/hepap/reports.shtm

3

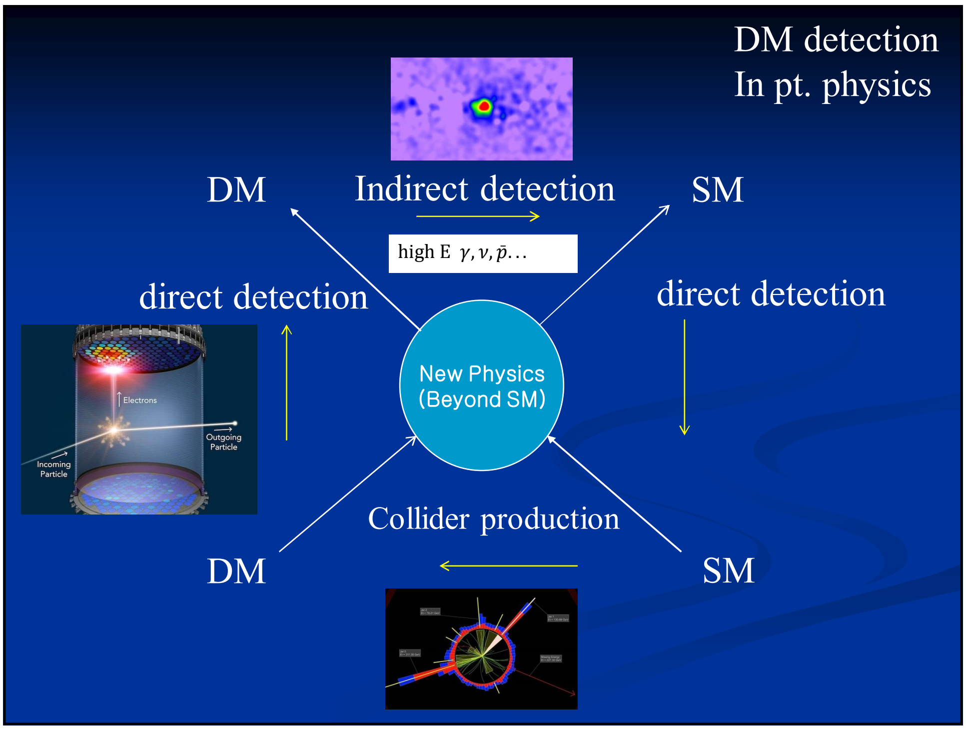
DM detection
In pt. physics
DM
Indirect detection
SM
high E $\gamma, \nu, \bar{p}\ldots$
direct detection
direct detection
New Physics
(Beyond SM)
Electrons
Incoming Particle
Outgoing Particle
Collider production
DM
SM

4

RESEARCH ARTICLE | PHYSICS

COSINE-100 full dataset challenges the annual modulation signal of DAMA/LIBRA

NELSON CARLIN, JAE YOUNG CHO, JAE JIN CHOI, SEONHO CHOI, ANTHONY C. EZERIBE, LUIS EDUARDO FRANÇA, CHANG HYON HA, IN SIK HAHN, SOPHIA J. HOLLICK, [...], AND GYUN HO YU +49 authors Authors Info & Affiliations

SCIENCE ADVANCES • 3 Sep 2025 • Vol 11, Issue 36 • DOI: 10.1126/sciadv.adv6503

205

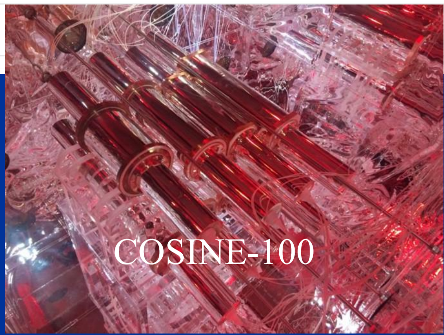

No direct, or indirect detection so far

5

Challenges for ΛCDM

cf) 2105.05208

•ΛCDM was very successful but is becoming non-standard?

1. Small scale crisis (on galactic scale and below)
   predicts too many small structures not observed

2. Hubble parameter tension ~5σ:
   H_0 mismatch between Planck estimation and SN

3. S_8 tension ~2-3σ : $S_8 \equiv \sigma_8\sqrt{\Omega_m/0.3}$, z < 2, Mpc
   matter density fluctuation amplitude mismatch between Planck estimation and WL & Cluster

4. DE is not Λ? ~4σ (ex, DESI, AP test)

5. Too early BHs and galaxies (Webb)

6. Cluster collision (collision speed & DM-star offset)

7. Li problem, Cosmic birefringence

…etc

→ ULDM model might address some of these tensions

6

Galaxies observed

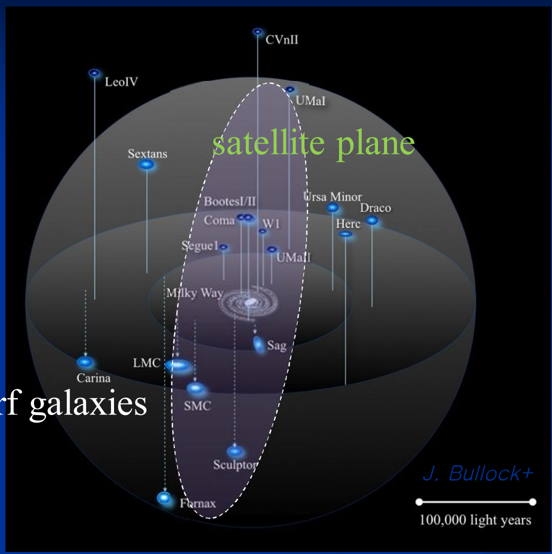

dwarf galaxies

Minimum mass
~ 10^6 Ms

Any good DM model should explain observed galaxies!

7

Solutions to Small scale problems

- CDM : m ~ GeV (can't solve the problems)
  → Baryon physics (SN, BH jets,…)

- WDM : m ~ keV
  → Catch 22 problem (cusp)
  Suppression of the power spectrum
  prohibiting the formation of the dwarf galaxy

- SIDM: $\sigma/m \sim 0.5\text{-}1\ \text{cm}^2/\text{g}$
  → velocity dependent?

- ULDM: $m \sim 10^{-22}$ eV
  → Lyman alpha favors $m > 10^{-21}$ eV ?

8

ULDM

- Galactic DM halo is a BEC made of ultralight scalar particles
- Quantum pressure (from uncertainty principle) prevents collapse like atoms
- Galaxy size ~ de Broglie wavelength of DM particles ~ kpc
  → m ~ 10^{-22} eV
- Small m → high # density → overlap of wave fn. → classical wave

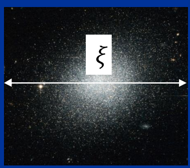

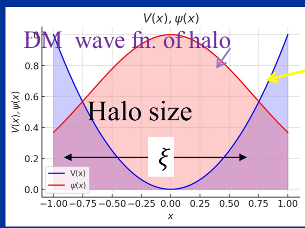

Self-gravitating potential well V

Schrodinger -Poisson (SP)

$$\begin{cases} i\hbar\partial_t\psi = -\frac{\hbar^2}{2m}\nabla^2\psi + mV\psi + int. \\ \nabla^2 V = 4\pi G(\rho_d + \rho_v) \end{cases}$$ visible, $\rho_d = m|\psi|^2$

ULDM SF $\phi(t,x) = \frac{1}{\sqrt{2m}}\left[e^{-imt}\psi(t,x) + e^{imt}\psi^*(t,x)\right]$

9

9

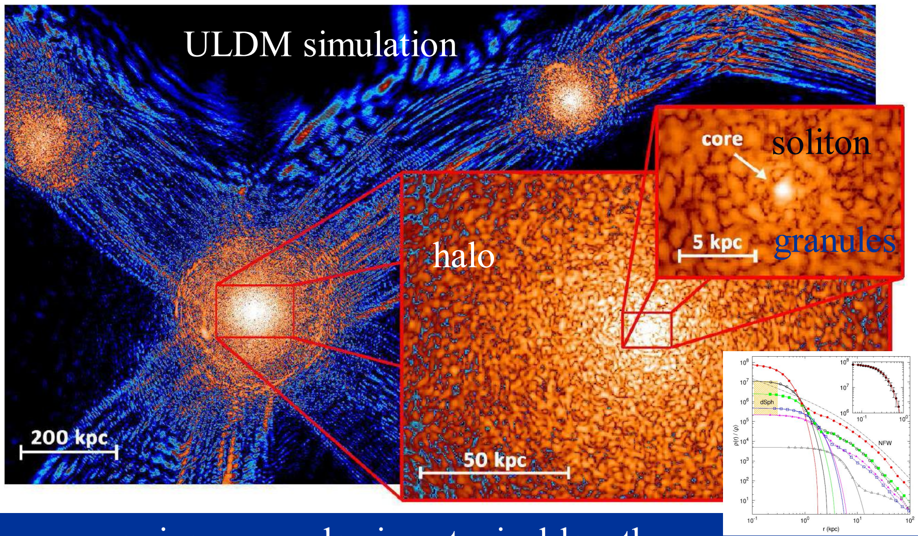

core size ~ granule size~ typical length

Schive etal , Nature physics 2014

10

10

Core/Cusp problem of CDM

Observation

ULDM simulation→
Core ~ de Broigle wave len.

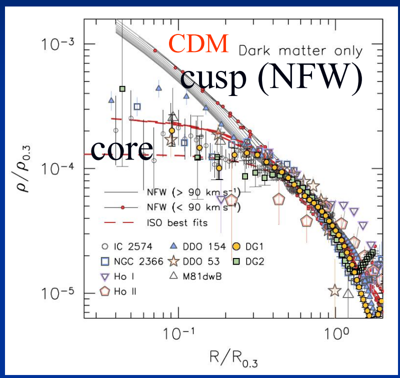

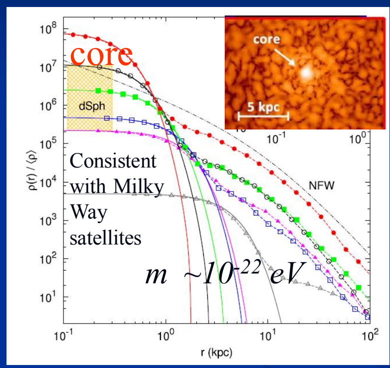

Schive etal , Nature physics 2014

Density profile from rotation curves of small galaxies strongly disfavors CDM
→ ULDM well explains the core profile!

11

Linear pert. Of ULDM

FDM has only 2 parameters m and bg density ρ_0 (or F)
(+ λ for ϕ^4 self-interacting ULDM)

a=scale factor

Nonrelativistic

$$i\hbar\left(\frac{\partial\psi}{\partial t}+\frac{3}{2}H\psi\right) = -\frac{\hbar^2}{2ma^2}\Delta\psi + mV\psi + \frac{\lambda|\psi|^2\psi}{2m^2}$$ self-int

Madelung representation

$$perturbation \quad \text{with } \psi = \sqrt{\rho}e^{iS}, \qquad v \equiv \frac{\hbar}{ma}\nabla S \Rightarrow$$

$$\begin{cases} \partial_t\rho + 3H\rho + \frac{1}{a}\nabla\cdot(\rho v) = 0 \\ \partial_t v + \frac{1}{a}v\cdot\nabla v + Hv + \frac{1}{\rho a}\nabla p + \frac{1}{a}\nabla V + \frac{\hbar^2}{2m^2a^3}\nabla\left(\frac{\Delta\sqrt{\rho}}{\sqrt{\rho}}\right) = 0 \end{cases}$$

Quantum Pressure

Density contrast (k space)

perturbation $\delta = \delta_k = \delta\rho/\rho_0$

$$\Rightarrow \partial_t^2\delta + 2H\partial_t\delta + \left(\left(\frac{\hbar^2k^2}{4m^2a^2} + c_s^2\right)\frac{k^2}{a^2} - 4\pi G\rho_0\right)\delta = 0$$

Hubble drag   gravity

Quantum Jeans length $\lambda_{QJ} = \frac{2\pi}{k_J}a = \pi^{3/4}\hbar^{1/2}(G\rho_0 m^2)^{-1/4} \propto 1/\sqrt{mH}$ ~ 10 kpc

- CDM-like on super-galactic scale (for a small $k < k_J$)
- Suppress sub-galactic structure (for a large $k > k_J$)

→ ULDM is an ideal alternative to CDM

12

12

Other cosmological Constraints

- BEC phase transition before nucleosynthesis: $m < 10^2$ eV
- field oscillation before equality $m > 10^{-28}$eV
- Maximum mass of galaxies from BS theory
  - spiral 1.04×10^{12}Ms < $O(1)\, M_p^2/m$ → $m < O(1)\ 1.28 \times 10^{-22}$eV
  - elliptical 1×10^{13}Ms < $O(1)\, M_p^2/m$ → $m < O(1)\ 1.28 \times 10^{-23}$eV
- Lyα forest $m > 10^{-21}$eV
- high-redshift galaxy luminosity → $m > 1.2 \times 10^{-22}$eV
- Stella subpopulations in Fornax → $m < 1.1 \times 10^{-22}$eV
- Ultra-faint dSphs → $m \sim 3.7\text{-}5.6 \times 10^{-22}$eV

fiducial value $m \sim 10^{-22}$eV

13

Scales from ULDM

$$\lambda_Q(z) = \frac{2\pi}{k} = \left(\frac{\pi^3\hbar^2}{Gm^2\bar\rho(z)}\right)^{1/4} = 71.75\ kpc\left(\frac{m}{10^{-22}\ eV}\right)^{-1/2}\left(\frac{\bar\rho}{10^{-7}M_\odot/pc^3}\right)^{-1/4} \propto (1+z)^{-3/4},$$

$$M_Q(z) = \frac{4\pi}{3}\left(\frac{\lambda_Q}{2}\right)^3\bar\rho = \frac{\pi^{\frac{13}{4}}}{6}\left(\frac{\hbar}{G^{\frac{1}{2}}m}\right)^{\frac{3}{2}}\bar\rho(z)^{\frac{1}{4}} = 1.93\times10^7\ M_\odot\left(\frac{m}{10^{-22}\ eV}\right)^{-3/2}\left(\frac{\bar\rho}{10^{-7}M_\odot/pc^3}\right)^{1/4} \propto (1+z)^{3/4},$$

Xc= $R_{99} = 9.95\left(\frac{\hbar}{m}\right)^2\frac{1}{GM} = 8.5\ kpc\left(\frac{10^{-22}eV}{m}\right)^2\frac{10^8M_\odot}{M},$ $t_c = \frac{1}{\sqrt{G\bar\rho}},$

$$a_c = x_c/t_c^2 = 0.0044\ G^3m^4M^3/\hbar^4 = 8.38\times10^{-14}\ meter/s^2\left(\frac{m}{10^{-22}eV}\right)^4\left(\frac{M}{10^8M_\odot}\right)^3 \simeq \sqrt{\frac{\hbar}{m}}(G\bar\rho)^{3/4},$$

$$v_c \equiv x_c/t_c = 0.21\ GMm/\hbar = 4.71\ km/s\left(\frac{M}{10^8M_\odot}\right)\left(\frac{m}{10^{-22}eV}\right) \simeq \sqrt{\frac{\hbar}{m}}(G\bar\rho)^{1/4},$$

$$\Sigma = 0.01\frac{G^2m^4M^3}{\hbar^4} = 1.38\ M_\odot/pc^2\left(\frac{m}{10^{-22}eV}\right)^4\left(\frac{M}{10^8M_\odot}\right)^4 \propto (1+z)^3$$

Ji& Lee JFOPA 2412.10285

14

core–halo relation of ULDM

$Q.Jeans\ mass$

$$M^{Q}{}_{J} = \frac{4\pi}{3}\rho(z)\lambda_{QJ}^{3}(z) = 1.204\times10^{8}\left(\frac{1+z}{m_{22}^{2}}\right)^{3/4}\left(\frac{\Omega_{\rm dm}}{0.27}\right)^{1/4}\left(\frac{h}{0.7}\right)^{1/2} M_{\odot}$$

$\sim M_h$ *halo mass*

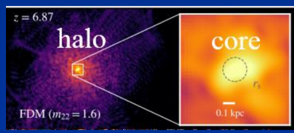

DM core size

$$r_s = 0.135 m_{22}^{-1}\left(\frac{\zeta'(z)}{\zeta'(7)}\right)^{-1}\left(\frac{M_h}{10^{11}M_{\odot}}\right)^{-1/3}\ \text{kpc}$$

DM core mass

$$M_s = 1.68\times10^{9} m_{22}^{-1}\left(\frac{\zeta'(z)}{\zeta'(7)}\right)\left(\frac{M_h}{10^{11}M_{\odot}}\right)^{1/3} M_{\odot} \sim \text{Mass gap}$$

where $m_{22} \equiv \frac{m}{10^{-22}\text{eV}}$, $\zeta' = (1+z)^{1/2}\zeta(z)^{1/6}$

with $\zeta(z) = (18\pi^2 + 82(\Omega_m(z)-1) - 39(\Omega_m(z)-1)^2)/\Omega_m(z) \sim 180$ at $z \geq 1$

15

GW background detected by pulsar timing array

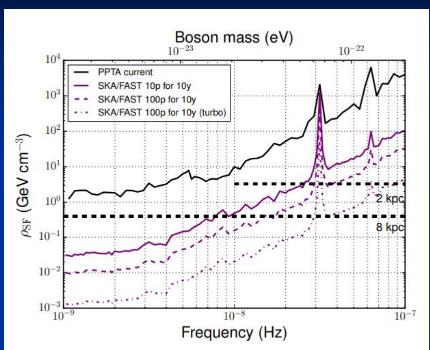

1810.03227

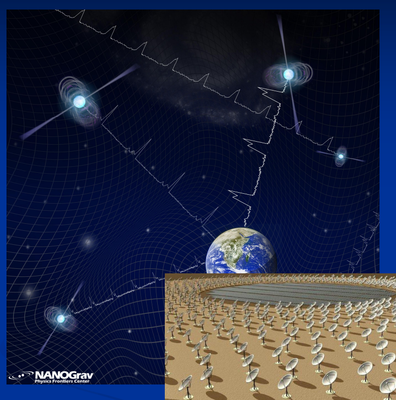

ULDM has
intrinsic osc time scale
1/m ~ yrs

$$\omega = \frac{1}{2.5months}\frac{m}{10^{-22}eV}$$

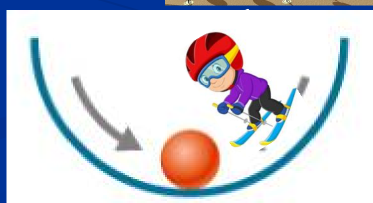

16

16

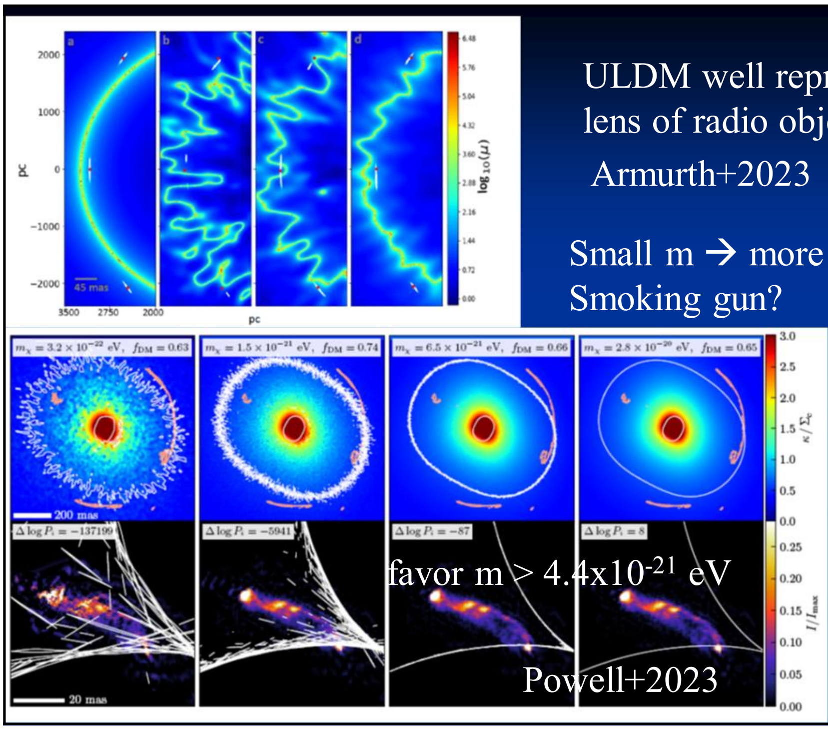

ULDM well reproduce lens of radio objects

Armurth+2023

Small m → more fuzzy

Smoking gun?

favor m > 4.4x10^{-21} eV

Powell+2023

17

17

Lyman alpha tension?

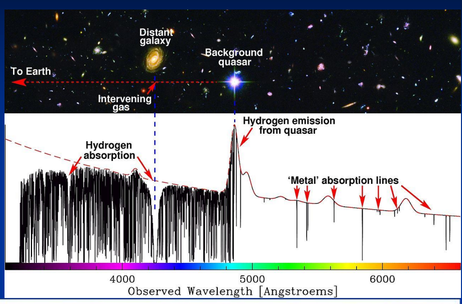

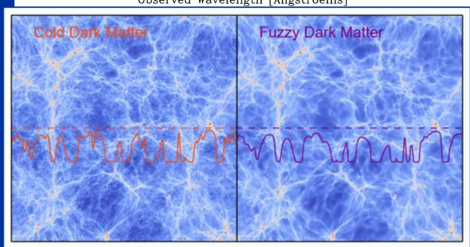

m > 10^{-21}eV

PRL 2017 (Irisic et al)

Hydrosimulation uncertainty is large

WDM (1, 3.3) keV ~ FDM (1, 20) x 10^{-22}eV

18

Gravitational atom

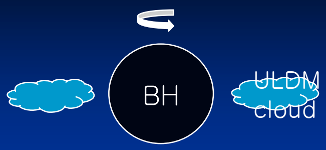

$$\left(g^{\alpha\beta}\nabla_\alpha\nabla_\beta - \mu^2\right)\Phi(t,r) = 0$$

ansatz $\quad \Phi(t,r) = \frac{1}{\sqrt{2\mu}}\left[\psi(t,r)e^{-i\mu t} + \psi^*(t,r)e^{i\mu t}\right]$

Schroedinger equation with a Coulomb-like central potential $\quad i\partial_t\psi(t,r) = \left(-\frac{1}{2\mu}\nabla^2 - \frac{\alpha}{r} + O(\alpha^2)\right)\psi(t,r)$

hydrogen atom like solution $\quad \psi_{nlm}(t,r) = R_{nl}(r)Y_{lm}(\theta,\phi)e^{i(\mu-\omega_{nlm})t}$

gravitational fine structure constant $\quad \alpha \equiv \frac{r_g}{\lambda_c} = \frac{GM\mu}{\hbar c} \approx 0.1\left(\frac{M}{10^{11}M_S}\right)\left(\frac{\mu}{10^{-22}\text{eV}}\right) << 1$

Occupation # is huge, presence of horizon

19

19

Superradiance
(Penrose process)

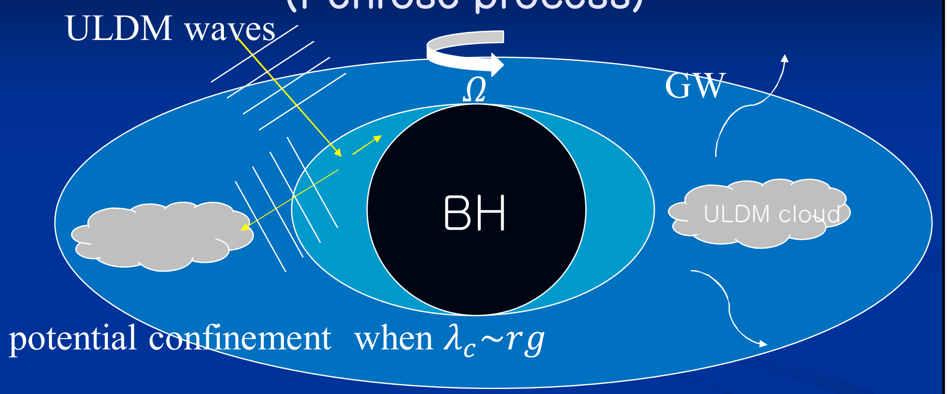

- growing mode if $\omega_{nlm} < m\Omega$ → BH spin decreases
  magnetic q. number
- can change GW patterns from a BH and BH binary

See Zhang & Yang 2018

20

20

UFD constraints

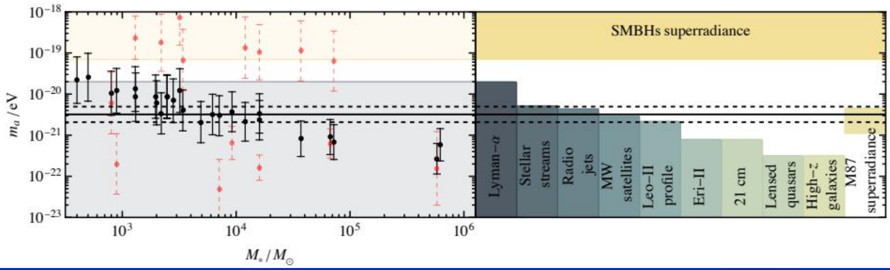

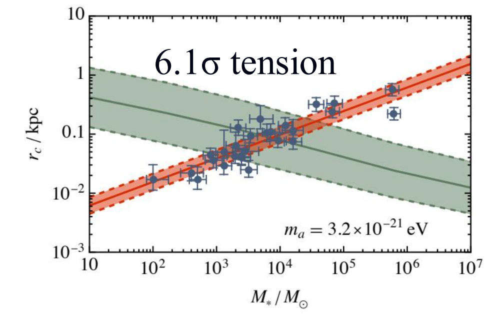

$$R_{99} = 9.95 \left(\frac{\hbar}{m}\right)^2 \frac{1}{GM}$$

Urrutia 2502.12030

21

Constraints on FDM (free ULDM) mass

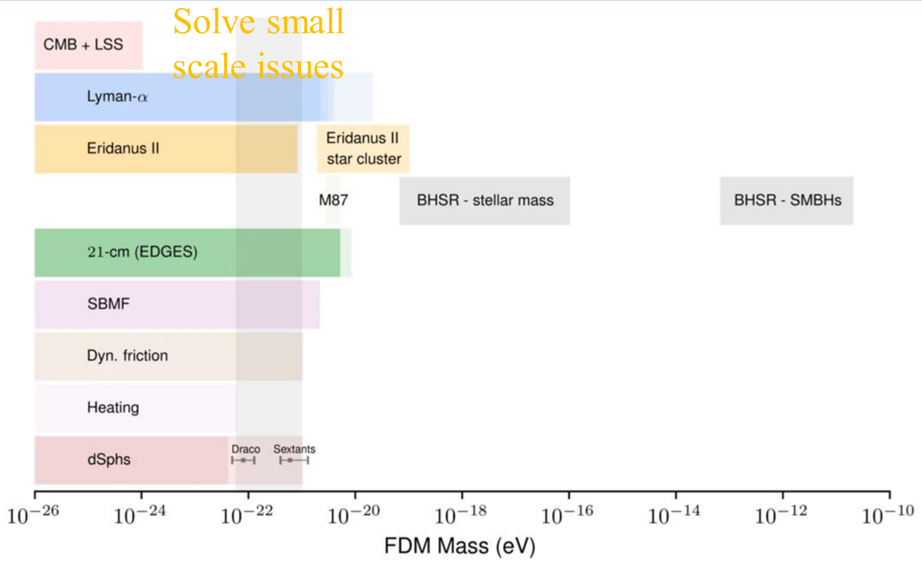

favors m > 10^{-21} eV?

MPA 22

22

Self-Interacting ULDM (SIULDM)

Lee and Koh (PRD 53, hep-ph/9507385)

Galactic DM halo is described by coherent scalar field with self-interaction

Action $S = \int \sqrt{-g} d^4x \left[\frac{-R}{16\pi G} - \frac{g^{\mu\nu}}{2}\phi^*_{;\mu}\phi_{;\nu} - \frac{m^2}{2}|\phi|^2 - \frac{\lambda}{4}|\phi|^4\right]$

Metric $ds^2 = -B(r)dt^2 + A(r)dr^2 + r^2 d\Omega$ *Spherical.*

Field $\phi(r,t) = (4\pi G)^{-\frac{1}{2}}\sigma(r)e^{-i\omega t}$

$$\tilde{m} \equiv \frac{m}{\lambda^{\frac{1}{4}}}$$

Exact ground state (soliton) $\sigma_* = \sqrt{\frac{\gamma_0 \, \mathrm{Sin}(\sqrt{2}r_*)}{\sqrt{2}r_*}}$

$r_* = r\Lambda^{-1/2}$

$\Lambda \equiv \frac{\lambda m_P^2}{4\pi m^2}$, $\Lambda >> 1$ (Newtonian & TF limit)

New constant length scale $RTF \approx \frac{\sqrt{\Lambda}}{m} = \sqrt{\frac{\pi\hbar^3\lambda}{8cGm^4}} \sim \sqrt{\tilde{m}}$

& *mass scale* $M_{\max} = \sqrt{\Lambda}\frac{m_P^2}{m}$

- Even tiny self-interaction drastically changes the scales!

→ allows wider range for m to fit observations

- $\tilde{m}$ determines all scales

23

23

Ji & Lee 2412.10285

Scales from SIULDM

$$\lambda_J = 2\pi\hbar\sqrt{\frac{a_s}{Gm^3}} = 2R_{TF} = \sqrt{\frac{\pi\hbar^3\lambda}{2cGm^4}} = 0.978\ kpc\left(\frac{\tilde{m}}{10eV}\right)^{-2},$$

$$\text{Xc=}\ R_{TF} = \pi\hbar\sqrt{\frac{a_s}{Gm^3}} = \sqrt{\frac{\pi\hbar^3\lambda}{8cGm^4}}.$$

$$t_c = \left(\frac{R_{TF}^3}{GM}\right)^{1/2} = \pi^{3/4}\left(\frac{\hbar^9\lambda^3}{512c^3G^5m^{12}}\right)^{1/4}\sqrt{\frac{1}{M}} \propto (1+z)^{-3/2}.$$

$$M_J(z) \equiv \frac{4\pi}{3}\left(\frac{\lambda_J}{2}\right)^3\bar{\rho} = \frac{4\pi^4\hbar^3}{3}\left(\frac{a_s}{Gm^3}\right)^{3/2}\bar{\rho} = \frac{\pi^{5/2}}{\sqrt{288}}\left(\frac{\hbar^3\lambda}{cGm^4}\right)^{3/2}\bar{\rho} = 49\,M_\odot\left(\frac{\tilde{m}}{10eV}\right)^{-6}\left(\frac{\bar{\rho}}{10^{-7}M_\odot/pc^3}\right) \propto (1+z)^3,$$

$$\rho_c = \frac{2\sqrt{2}M\left(\frac{cGm^4}{\lambda}\right)^{3/2}}{\hbar^{9/2}\pi^{3/2}} = 0.106\ M_\odot/pc^3\left(\frac{\tilde{m}}{10\ eV}\right)^6\left(\frac{M}{10^8M_\odot}\right) \propto (1+z)^3,$$

$$a_c = \mathrm{x}_c/t_c^2 = \frac{16cG^2m^4M}{\pi\hbar^3\lambda} = 1.163\times10^{-10}\ meter/s^2\left(\frac{\tilde{m}}{10eV}\right)^4\left(\frac{M}{10^8M_\odot}\right) \propto (1+z)^3$$

$$\Sigma = \frac{\hbar\pi^{3/2}\sqrt{\frac{\hbar\lambda}{cGm^4}}\bar{\rho}}{6\sqrt{2}} = 5.124\ M_\odot/pc^2\left(\frac{\tilde{m}}{10eV}\right)^{-2}\left(\frac{\bar{\rho}}{10^{-2}M_\odot/pc^3}\right) = 104.4\ M_\odot/pc^2\left(\frac{\tilde{m}}{10eV}\right)^{-2}\left(\frac{M}{10^8M_\odot}\right) \propto (1+z)^3$$

24

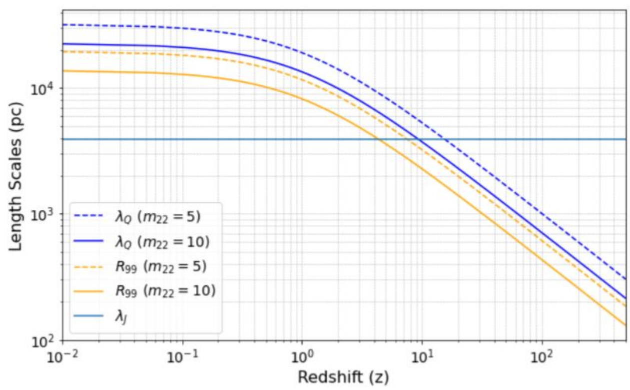

FIG. 1: The evolution of the typical length scales of galaxies versus redshift z. The upper two curves represent λ_Q for $m_{22} = m/10^{-22}eV = 5$ and $m_{22} = 10$, respectively, while the lower two curves represent the corresponding R_{99}. The horizontal line represents $\lambda_J = 2R_{TF}$ in the TF limit with $\tilde{m} = 5\ eV$. When $\lambda_J > \lambda_Q$, the size and mass of a dark matter halo formed at that time are governed by self-interaction-induced repulsion rather than quantum pressure, especially at high redshifts $z \gg 10$ and for larger mass $m \gtrsim 10^{-21}\ eV$. We expect galaxy density perturbations to begin collapsing in the redshift range $O(10) \lesssim z \lesssim O(100)$.

Ji & Lee 2412.10285

25

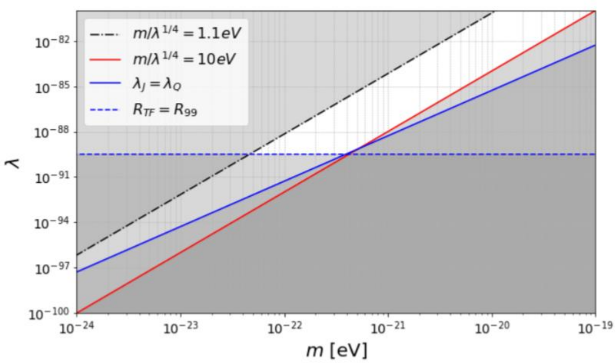

FIG. 2: Cosmological constraints on the mass m and coupling constant λ of ULDM are shown. The gray region denotes the parameter space excluded by current constraints. The dash-dot line corresponds to the bound from the dark matter density Ω_ϕ (Eq. (36)). The red solid line indicates the observational constraint from galaxies, $\tilde{m} \lesssim 10$ eV. The blue line marks the boundary where the condition $\lambda_J > \lambda_Q$ (Eq. (23)) holds at redshift $z = 100$. The dashed horizontal line represents the condition $R_{TF} > R_{99}$ for a soliton mass of $M = 10^8\ M_\odot$.

26

Alberto Diez-Tejedor etal PRD 2014

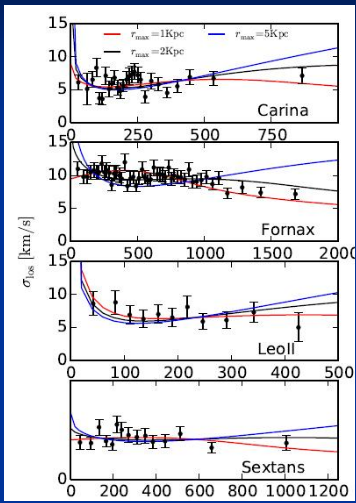

$$\lambda^{1/2}\left(\frac{m_P}{m}\right)^2 \geq 10^{50} \to \left(\frac{m_P}{10^{25}}\right) \approx 1221eV \geq \frac{m}{\lambda^{1/4}}$$

$$\rho = \sigma^2 = \rho_0 \frac{\sin(\pi r / r_{max})}{\pi r / r_{max}}$$

$$r_{max} \equiv \sqrt{\frac{\pi^2 \Lambda}{2}} \simeq 49\left(\frac{\lambda^{1/4}}{m / eV}\right)^2 kpc$$

dSphs $\quad r_{max} \sim 1kpc \to m / \lambda^{1/4} \sim 7eV$

27

Li etal 1310.6061

Cosmological evolution

$$V(\psi) = \frac{1}{2}mc^2|\psi|^2 + \frac{\lambda}{2}|\psi|^4$$

$$\langle \bar{w} \rangle \equiv \frac{\langle \bar{p} \rangle}{\langle \bar{\rho} \rangle} = \frac{1}{3}\left[\frac{1}{1 + \frac{2mc^2}{3\lambda\langle|\psi|^2\rangle}}\right]$$

Time varying Eq. of state

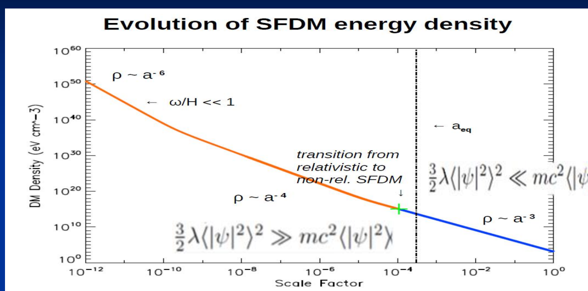

$\frac{3}{2}\lambda\langle|\psi|^2\rangle^2 \gg mc^2\langle|\psi|^2\rangle$

$\frac{3}{2}\lambda\langle|\psi|^2\rangle^2 \ll mc^2\langle|\psi|^2\rangle$

1) Z_eq=3390

$$\frac{\lambda}{(mc^2)^2} \leq 4 \times 10^{-17} \text{ eV}^{-1} \text{ cm}^3.$$

$\Rightarrow m^4/\lambda > 4.7 \times 10^{-7} eV^4$

2) Big Bang Nucleosynthesis

$$\frac{\Delta N_{eff}}{N_{eff,\text{standard}}} = \frac{3.71^{+0.47}_{-0.45} - 3.046}{3.046} = \frac{\rho_{SFDM}}{\rho_\nu}$$

$$9.5\times 10^{-19} \text{ eV}^{-1} \text{ cm}^3 \leq \lambda/(\text{mc}^2)^2 \leq 1.5\times 10^{-16} \text{ eV}^{-1} \text{ cm}^3$$

$$\to 2.6eV \leq \frac{m}{\lambda^{1/4}} \leq 9.5eV$$

28

28

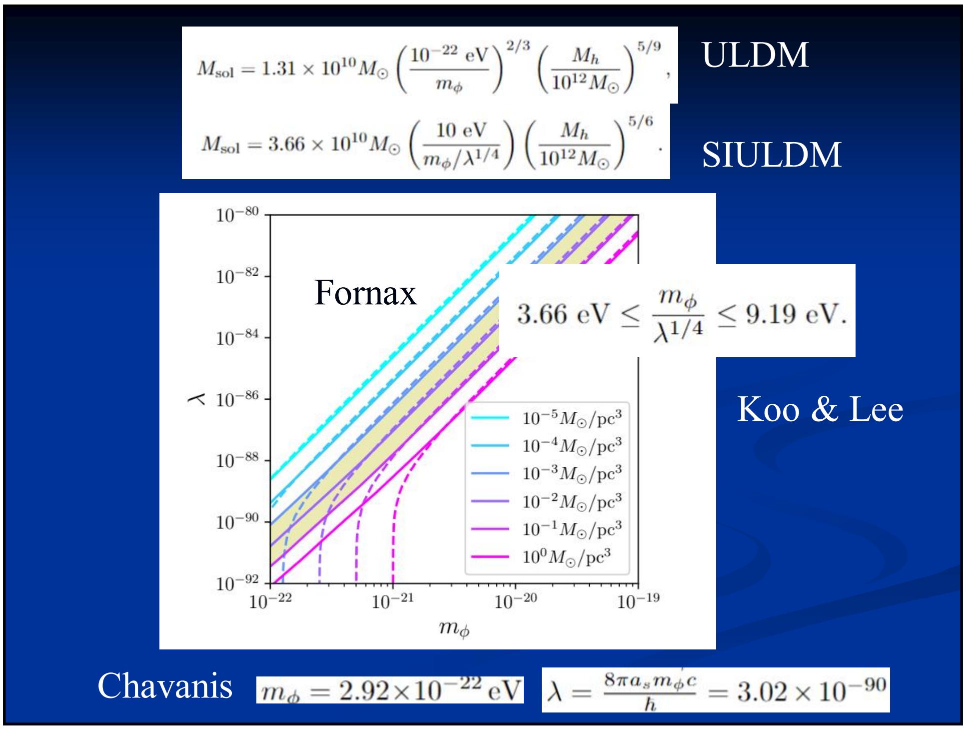

$M_{sol} = 1.31 \times 10^{10} M_\odot \left(\frac{10^{-22}\ eV}{m_\phi}\right)^{2/3} \left(\frac{M_h}{10^{12} M_\odot}\right)^{5/9}$,
ULDM
$M_{sol} = 3.66 \times 10^{10} M_\odot \left(\frac{10\ eV}{m_\phi/\lambda^{1/4}}\right) \left(\frac{M_h}{10^{12} M_\odot}\right)^{5/6}$.
SIULDM
Fornax
$3.66\ eV \le \frac{m_\phi}{\lambda^{1/4}} \le 9.19\ eV.$
Koo & Lee
$10^{-5} M_\odot/pc^3$
$10^{-4} M_\odot/pc^3$
$10^{-3} M_\odot/pc^3$
$10^{-2} M_\odot/pc^3$
$10^{-1} M_\odot/pc^3$
$10^{0} M_\odot/pc^3$
λ
m_ϕ
Chavanis
$m_\phi = 2.92 \times 10^{-22}\ eV$
$\lambda = \frac{8\pi a_s m_\phi c}{\hbar} = 3.02 \times 10^{-90}$

29

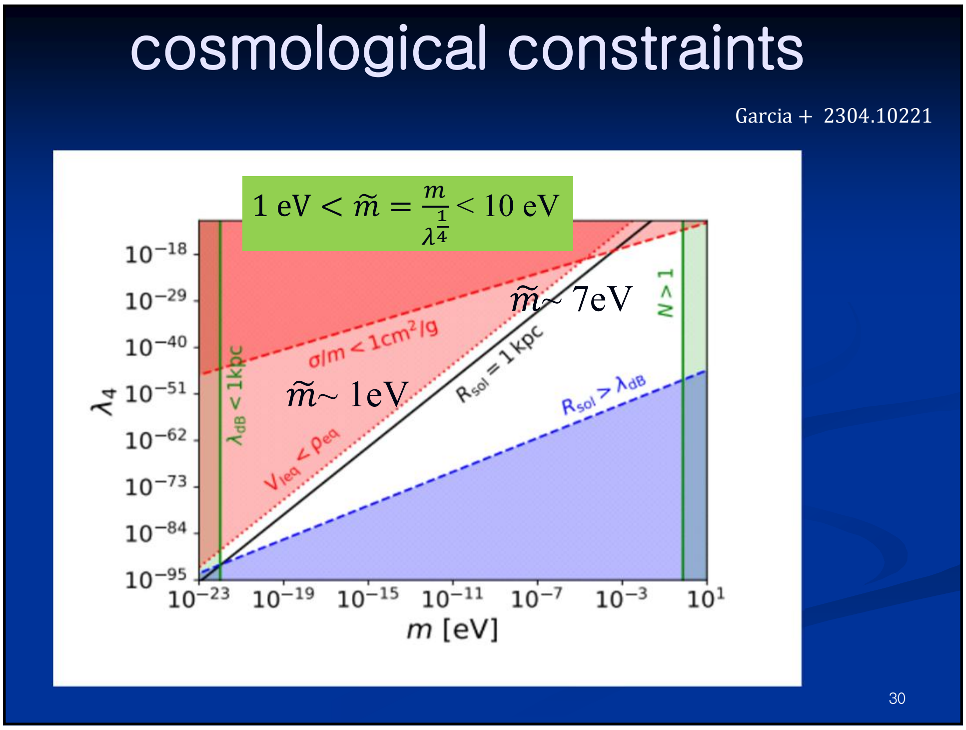

cosmological constraints
Garcia + 2304.10221
$1\ eV < \tilde{m} = \frac{m}{\lambda^{\frac{1}{4}}} < 10\ eV$
$\tilde{m}\sim 7eV$
$\tilde{m}\sim 1eV$
$\sigma/m < 1 cm^2/g$
$R_{sol} = 1\ kpc$
$R_{sol} > \lambda_{dB}$
$\lambda_{dB} < 1 kpc$
$V_{leq} < \rho_{eq}$
$N > 1$
λ_4
m [eV]
30

30

ULDM detection

ULDM makes coherent waves → if coupled to EM field
→ change in effective coupling constants (fine structure)
→ oscillation in frequency

sinusoidal modulation

$$\frac{1}{4g^2} F_{\mu\nu}F^{\mu\nu} + \frac{\varphi d_e}{4g^2} F_{\mu\nu}F^{\mu\nu}$$

$$\alpha(t) \approx \alpha\,[1 + d_e \varphi_0 \cos(\omega t + \delta)]$$

$$\rho_\varphi = \frac{1}{2} m^2 \varphi^2 = 0.3\mathrm{GeV/cm}^3$$

similar to 5th force

$$\omega = \frac{1}{2.5 months} \frac{m}{10^{-22} eV}$$

Arvanitaki et al., PRD 91

31

detection by atomic clock

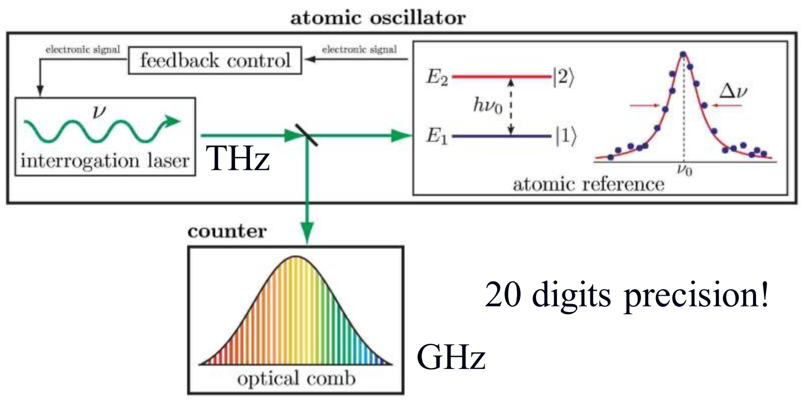

20 digits precision!

Fig. 2. – Schematic view of an optical atomic clock: the local oscillator (laser) is resonant with the atomic transition. A correction signal is derived from atomic spectroscopy that is fed back to the laser. An optical frequency synthesizer (optical frequency comb) is used to divide the optical frequency down to countable microwave or radio frequency signals.

arXiv:1401.2378v2

32

Nuclear Clock

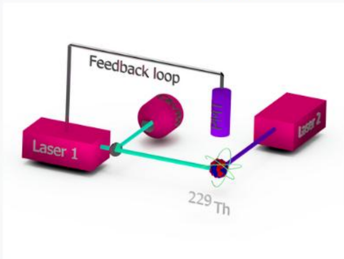

Concept of a thorium-229 based nuclear optical clock.

Thorium-229's uniquely low-energy nuclear isomer transition at about 8.3 eV (≈150 nm, ~2×10^{15} Hz) makes it the only nuclear excitation accessible to laser spectroscopy and thus a prime candidate for a nuclear optical clock.

33

detection

Oscillation of fine structure constant

$$\alpha(t) \approx \alpha\ [1 + d_e \varphi_0 \cos(\omega t + \delta)]$$

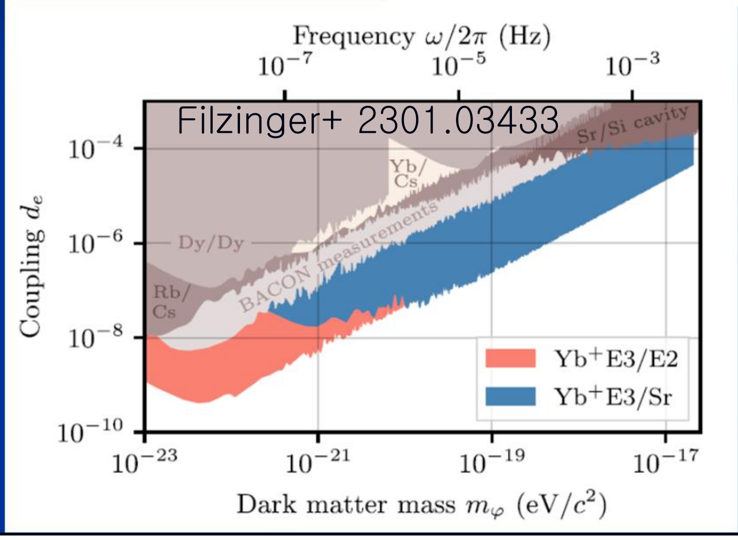

34

$\phi(t,\vec{x}) = \phi_0 \cos(m_\phi t - \vec{k}_\phi \cdot \vec{x} + \alpha)$ is

$$V = M\left[1 + \alpha_M \kappa \phi(t,\vec{x})\right] \simeq M\left[1 + d_g \kappa \phi(t,\vec{x})\right],$$

$$\mathcal{L}_\phi = \kappa\phi\Big[+\frac{d_e}{4e^2}F_{\mu\nu}F^{\mu\nu} - \frac{d_g\beta_3}{2g_3}G^A_{\mu\nu}G^{A\mu\nu} - d_{m_e}m_e\bar{e}e - \sum_{i=u,d}(d_{m_i}+\gamma_{m_i}d_g)m_i\bar{\psi}_i\psi_i\Big], \quad (2)$$

$$\delta\lambda_{\phi,\mathrm{SM}} \sim +\frac{(d_{m_i}\kappa m_i)^4}{16\pi^2} \sim +10^{-92}\left(\frac{d_{m_t}}{10^{-6}}\right)^4$$

$$\kappa \equiv \frac{\sqrt{4\pi}}{M_{\rm Pl}},$$

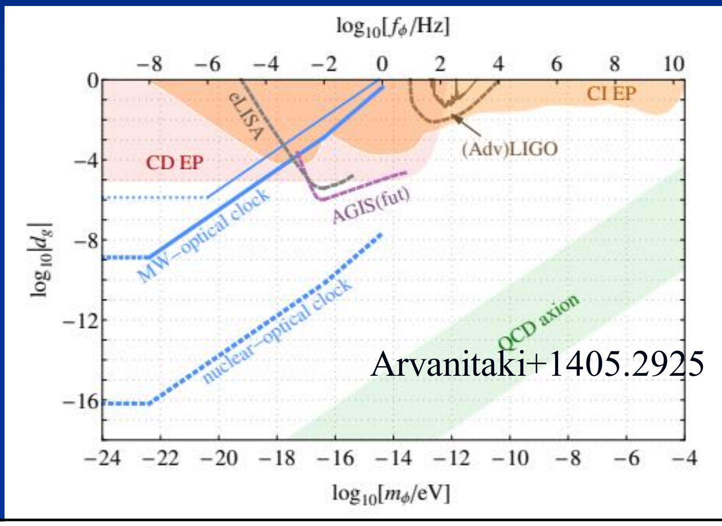

35

Cross section

$\sigma(\phi\phi \to \phi\phi) = \lambda^2/128\pi m^2$

$\frac{\sigma}{m} = \frac{\lambda^2}{128\pi m^3} \approx 1\ cm^2 g^{-1}$ for galactic cluster

a cosmological constraint

$if\ m{\sim}10^{-22}eV \to \lambda{\sim}10^{-92}$

$\frac{m}{\lambda^{1/4}} \sim 0.1\mathrm{eV}$

One loop correction

if gauge interaction, $g\,A_\mu\phi$

effective self−int. coupling $\lambda' {\sim}\, O(\frac{3g^4}{64\pi^2})$

$\lambda' < \lambda_{obs} \Rightarrow g \leq 10^{-22.5} \Rightarrow d_e {\sim}\, g^2 \leq 10^{-45}$

→ gauge coupling should be extremely small

→ hard to direct detect, if not impossible

in preparation

36

36

GW

2501.08930

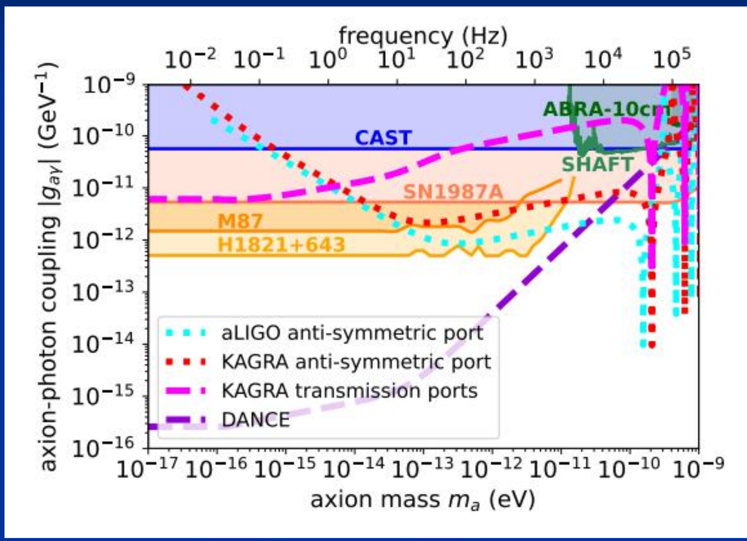

37

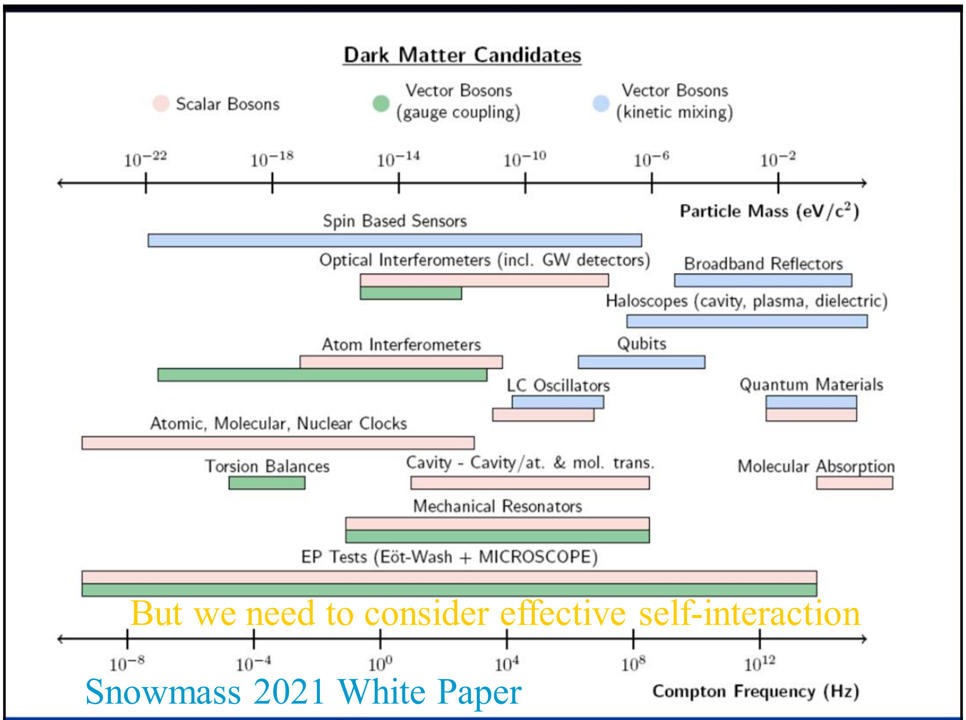

But we need to consider effective self-interaction

Snowmass 2021 White Paper

38

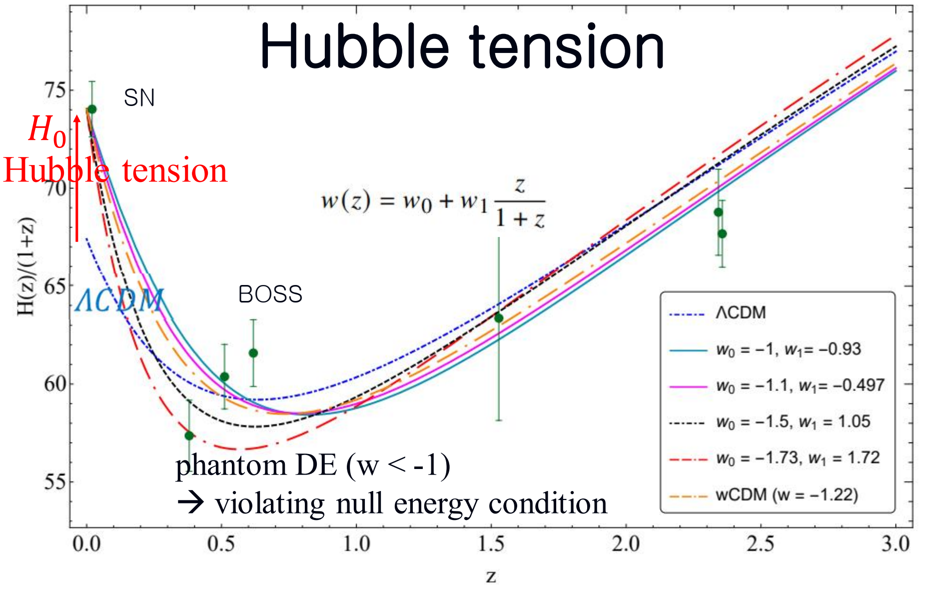

Alestas & L. Perivolaropoulos 2021 39

39

H_0 estimation from CMB

$\theta_s = \frac{r_s}{D_A}$ is a standard ruler with 0.04% precision. (fixed)

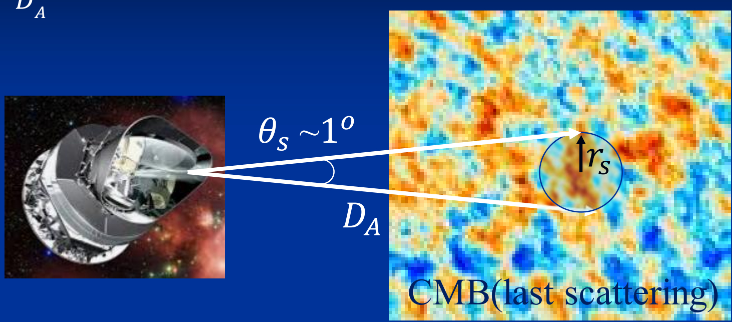

Sound Horizon $r_s = \frac{c}{\sqrt{3}H_{ls}} \int_{z_{ls}}^{\infty} \frac{dz}{[\rho(z)/\rho(z_{ls})]^{1/2}(1+R(z))^{1/2}}$

Angular distance $D_A = \frac{c}{H_0} \int_0^{z_{ls}} \frac{dz}{[\rho(z)/\rho_0]^{1/2}} \sim \frac{1}{H_0}$

r_s & D_A depend on expansion history (matter contents $\rho(z)$)

40

$$H_0 = \theta_s H_{ls} \frac{\int_{z_{ls}}^{0} \frac{c\,dz}{[\rho(z)/\rho_0]^{1/2}}}{\int_{\infty}^{z_{ls}} \frac{c_s(z)\,dz}{[\rho(z)/\rho(z_{ls})]^{1/2}}}$$

late time (decrease $\rho(z)$)

early time (increase $\rho(z)$)

To increase H_0 we can ($\theta_s = \frac{r_s}{D_A}$ $fixed$)

1) in early time solutions (decrease r_s to decrease D_A)

• increase $\rho(z)$ (extra radiation, EDE) just before ls
→ but need more perturbation
→ worsen S_8 tension, ad hoc matter, coincidence?

$$D_A = \frac{c}{H_0}\int_0^{z_{ls}} \frac{dz}{[\rho(z)/\rho_0]^{1/2}}$$

2) in late time solutions (r_s & D_A fixed, increase the integral)

• decrease $\rho(z)$ by decaying DM after ls and/or increase DE to increase the integral
→ late evolution changes
→ tensions with BAO, SN; null energy violation; fine tuning

Do we need both solutions?

41

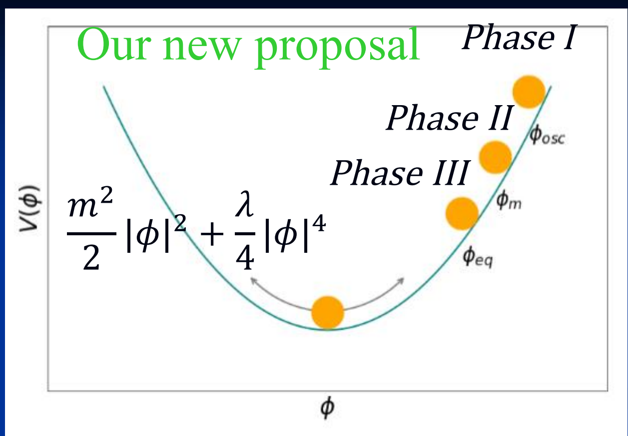

JLee 2502.11568

$V(\phi) \propto \phi^n$ decays with an equation of state $w = \frac{(n-2)}{(n+2)}$

$$\begin{cases} DE-like\ (slow-roll)\ for\ z_{osc} < z\ (Phase\ I) \\ Dark\ rad\text{-}like\ (\phi^4 > \phi^2)\ or\ z_m < z < z_{osc}\ (Phase\ II) \\ \text{CDM}\ (\phi^4 < \phi^2)\ \text{or}\ z < z_m\ (Phase\ III) \end{cases}$$

SIULDM alone is enough!

42

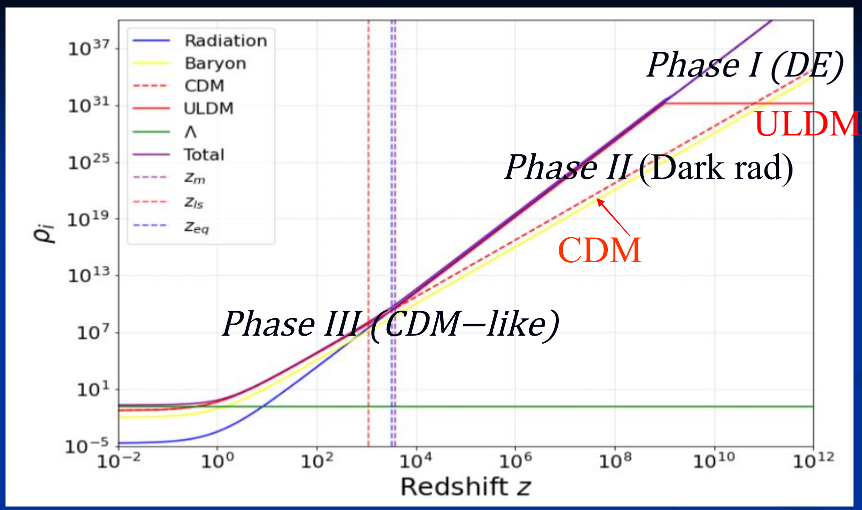

→ SIULDM acts as a natural extra radiation comp. just before ls

→ We don't need exotic matter or fine tuning?

43

$$\frac{H_0(ULDM)}{H_0(CDM)} \simeq \frac{\int_{z_{ls}}^{\infty} \rho(CDM)(z)^{-1/2} \frac{dz}{\sqrt{1+R(z)}}}{\int_{z_{ls}}^{\infty} \rho(ULDM)(z)^{-1/2} \frac{dz}{\sqrt{1+R(z)}}}$$

$$\omega_i = h^2 \Omega_i$$

$$\rho(ULDM)(z) \propto \begin{cases} \sqrt{\omega_r(1+z)^4 + \omega_m(1+z)^3 + \omega_\Lambda} & for\, z < z_m \text{ (Phase III)} \\ \sqrt{\omega_r(1+z)^4 + \omega_\phi \frac{(1+z)^4}{1+z_m} + \omega_b(1+z)^3 + \omega_\Lambda} & for\, z_m < z < z_{osc} \text{ (Phase II)} \\ \sqrt{\omega_r(1+z)^4 + \omega_b(1+z)^3 + \omega_\phi \frac{(1+z_{osc})^4}{1+z_m} + \omega_\Lambda} & for\, z_{osc} < z \text{ (Phase I)} \end{cases}$$

where $\omega_b = 0.022, \omega_\phi = 0.119, \omega_r = 4.2 \times 10^{-5}, \omega_\Lambda = 0.314$ from Planck's Λ CDM values

Using the densities, we numerically obtain $\frac{H_0(\text{ULDM})}{H_0(\text{CDM})} \simeq 1.049$ for $\tilde{m} = 0.9$

$*$ $\tilde{m}$ is near lower bound, input data assumed ΛCDM, age problem?

44

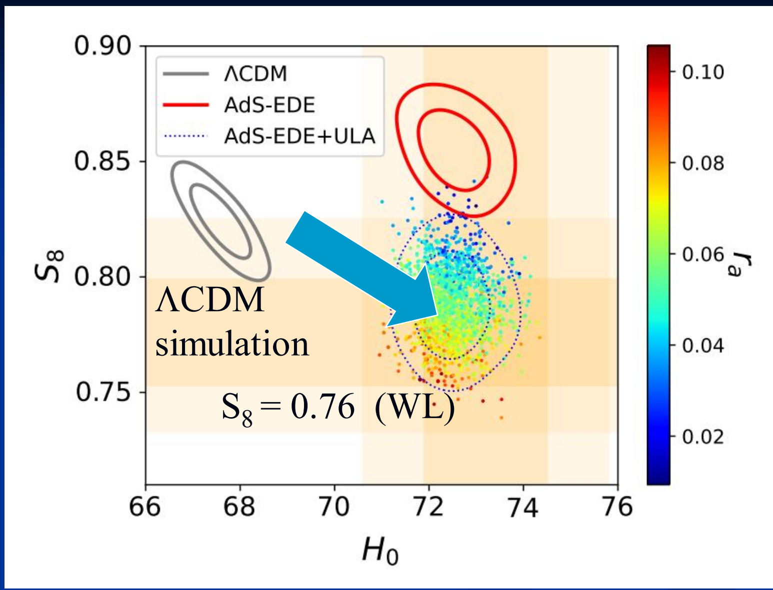

Can ULDM solve both H_0 and S_8 ? Ye+ 2107.13391

→ need extra DE & ULDM with $m < 10^{-24}$ eV

45

45

Conclusions

ULDM with m~10^{-21} eV or

self-interacting ULDM with $\frac{m}{\lambda^{1/4}} \sim 1 eV$

seems to be a viable alternative to CDM

46